🌐 Thieme

Practical Aspects of novel MRI Techniques in Neuroradiology: Part 2 – Acceleration Methods and Implications for Individual Regions

Praktische Aspekte neuerer MRT-Techniken in der Neuroradiologie: Teil 2 – Beschleunigungsverfahren und Regionen-spezifische Implikationen

Authors

Benedikt Sundermann[1, 2, 3] 🆔, Benoit Billebaut[3, 4], Jochen Bauer[3] 🆔, Catalin George Iacoban[1], Olga Alykova[1], Christoph Schülke[5], Maike Gerdes[1], Harald Kugel[3], Sojan Neduvakkattu[3], Holger Bösenberg[1], Christian Mathys[1, 2, 6]

Affiliations

1 Institute of Radiology and Neuroradiology, Evangelisches Krankenhaus, Medical Campus University of Oldenburg, Germany
2 Research Center Neurosensory Science, University of Oldenburg, Germany
3 Clinic for Radiology, University Hospital Münster, Germany
4 School for Radiologic Technologists, University Hospital Münster, Germany
5 Radiologie Salzstraße, Münster, Germany
6 Department of Diagnostic and Interventional Radiology, University of Düsseldorf, Germany

Correspondence

PD Dr. Benedikt Sundermann
Institut für Radiologie und Neuroradiologie, Evangelisches Krankenhaus Oldenburg, Steinweg 13–17, 26122 Oldenburg, Germany
Tel.: +49/4 41/2 36 97 54
benedikt.sundermann@uni-oldenburg.de

🌐 Supplementary material is available under https://doi.org/10.1055/a-1800-8789

ABSTRACT

Background Recently introduced MRI techniques facilitate accelerated examinations or increased resolution with the same duration. Further techniques offer homogeneous image quality in regions with anatomical transitions. The question arises whether and how these techniques can be adopted for routine diagnostic imaging.

Methods Narrative review with an educational focus based on current literature research and practical experiences of different professions involved (physicians, MRI technologists/radiographers, physics/biomedical engineering). Different hardware manufacturers are considered.

Results and Conclusions Compressed sensing and simultaneous multi-slice imaging are novel acceleration techniques with different yet complimentary applications. They do not suffer from classical signal-to-noise-ratio penalties. Combining 3D and acceleration techniques facilitates new broader examination protocols, particularly for clinical brain imaging. In further regions of the nervous systems mainly specific applications appear to benefit from recent technological improvements.

Key points:
- New acceleration techniques allow for faster or higher resolution examinations.
- New brain imaging approaches have evolved, including more universal examination protocols.
- Other regions of the nervous system are dominated by targeted applications of recently introduced MRI techniques.

Citation Format
- Sundermann B, Billebaut B, Bauer J et al. Practical Aspects of novel MRI Techniques in Neuroradiology: Part 2 – Acceleration Methods and Implications for Individual Regions. Fortschr Röntgenstr 2022; 194: 1195–1203

ZUSAMMENFASSUNG

Hintergrund Neuere MR-Techniken ermöglichen unter anderem, Untersuchungen deutlich zu beschleunigen oder in gleicher Zeit höher aufgelöste Bilddaten aufzunehmen und

Übergangsregionen mit homogener Bildqualität zu untersuchen. Es stellt sich die Frage nach der breiten Anwendbarkeit solcher Techniken in der Routinediagnostik.

Methode Narrative Übersichtsarbeit mit Fortbildungsschwerpunkt basierend auf aktueller Literaturrecherche und praktischen Erfahrungen verschiedener Berufsgruppen (ärztliches Personal, MTRA, MR-Physik/Technik) und mit Geräten unterschiedlicher Hersteller.

Ergebnisse und Schlussfolgerungen Mit Compressed Sensing und simultaner Mehrschicht-Bildgebung stehen neue Beschleunigungsverfahren zur Verfügung, die sich in ihren Einsatzmöglichkeiten unterscheiden und ergänzen. Sie weisen keine klassischen Einschränkungen des Signal-Rausch-Verhältnisses auf. Die Kombination von verbesserten 3D- und Beschleunigungstechniken ermöglicht insbesondere bei der Bildgebung des Gehirns neue universelle Untersuchungsprotokolle, während in anderen Regionen des Nervensystems vor allem spezifische Indikation von neuen Methoden profitieren.

Introduction

Newer techniques are currently fundamentally changing imaging strategies in magnetic resonance imaging (MRI). In this part, recent acceleration techniques will be presented first, followed by an outlook on other new techniques and an overview of possible routine applications in neuroradiology of the techniques presented in Parts 1 and 2.

Techniques

New Acceleration Techniques

Conventional acceleration techniques such as parallel imaging, both in image space (e. g., SENSE[1]) and in k-space (e. g., GRAPPA and the further developed CAIPIRINHA), are accompanied by a reduction in signal-to-noise ratio (SNR) inhomogeneously distributed across the image [1]. Newer techniques allow acceleration without this typical SNR limitation.

Simultaneous Multi-slice Imaging

Technical background and potential advantages

In conventional 2D sequences, individual slices are excited and recorded separately. In simultaneous multi-slice (SMS) or multiband techniques, special high-frequency pulses are used to excite several slices simultaneously and then read them out [2]. Parallel imaging principles are used to separate the signals from the different slices [2, 3]. Theoretically, acceleration is not accompanied by reduced SNR [2]. Depending on the manufacturer, SMS is available for echoplanar imaging (EPI) as well as 2D turbo spin echo (TSE) [2]. Further reading: [2].

Possible limitations

Even if the SNR is theoretically not significantly negatively affected by SMS acceleration, the achievable acceleration is limited. Thus, the TR cannot be reduced indefinitely depending on the weighting (and thus the measurement time) and this in turn affects the SNR [4]. In addition, ghosting and so-called slice-leakage artifacts [2, 5–8] as well as crosstalk [2, 9] can occur (▶ **Fig. 1**). The latter can significantly reduce image quality. They are related to the SMS acceleration factor, the number of slices and the FOV shift factor [2, 3]. Although the occurrence of slice crosstalk can be theoretically inferred [2], it is difficult for the clinical user to predict its appearance.

Practical notes on application

Activating SMS does not automatically cause acceleration. Rather, it becomes possible for the user to reduce the repetition time (TR) and thus shorten the measurement time.

Other practical considerations include the choice of receiving coil, slice orientation, and a suitable acceleration factor. Since slice separation is based on similar principles to parallel imaging, it is necessary to have multiple coil elements along the slice stack (increasingly with higher acceleration factor). When recording transverse slices, it should be noted that the number of coil elements is often relatively small for this direction. For example, with 20-channel head coils with SMS for transverse slices, acceleration by a factor of 2 is usually possible, whereas SMS acceleration factors of 8, used e. g. in scientific applications with 64-channel coils (cf. [8, 10–12]), are not realistic with current clinical hardware. In the scientific literature, it is predominantly recommended to achieve acceleration with SMS alone [12] because additional use of parallel imaging within the slice is less efficient in terms of artefacts and SNR. However, for clinical coils, it may be useful to combine an SMS factor of 2 with a low factor of parallel imaging within the slice [13]. At the same time, coil elements should be activated generously, even if they only slightly overlap with the scan region.

In our opinion, SMS sequences can contribute to significantly faster examinations or better image quality when routine protocols are specifically optimized. SMS sequences in routine protocols should be designed to anticipate sufficient slices (as integer multiples of the acceleration factor) to prevent artefact generation due to spontaneous increase of the number of slices by users.

---

1 In some instances trade names are provided in this article for user orientation because there is no uniform non-proprietary name concept for MR techniques as in pharmacology. In contrast to other abbreviations, acronyms which primarily have the character of a product or proper name are not listed here for better readability. Some of these are trademarks of the respective manufacturers. The naming also partly reflects the practical experiences of the authors. In particular, designation is not intended to give preference to any specific manufacturer and its implementations, nor to infringe upon any corresponding trademark rights.
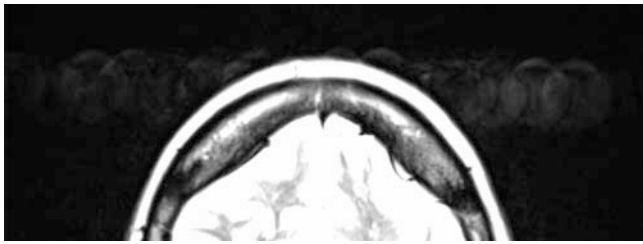
► **Fig. 1** 2 D T2 TSE with simultaneous multi-slice imaging in transverse slice orientation. Contrast settings were chosen to highlight the artefact. Example of a slice leakage artefact: In this case eye movement artefacts are additionally visible in a slice well above the orbits. Such artefacts can alter image contrast in distant slices and in rare cases mimic lesions; thus, knowledge of this artefact is important.

Compressed Sensing

Technical background and potential advantages

An analogy that can be used to better understand the idea of compressed sensing (CS) is the compression of image data. An image file can be reduced in size by omitting redundant or less relevant information without causing a relevant change in the visual impression [14]. What would it be like if images could be captured in such a compressed form right from the start and thus significantly save measurement time? CS approaches this goal by combining incoherent undersampling with iterative reconstruction of image data [15, 16]. An intermediate step is a transfer of the data into a sparse representation, usually using a wavelet transform [15]. In theory, applications that benefit most from CS are those that are sparse anyway (i. e., contain mostly black-and-white information) or are easier to convert to such a representation due to redundancy (e. g., 3 D sequences and dynamic measurements with many phase-encoding steps, the number of which can be reduced by undersampling). Furthermore, CS can be combined with conventional parallel imaging as well as noise reduction [17]. CS is an umbrella term for a family of these approaches. Evaluations of routine clinical applications suggest that CS is very unlikely to be inferior to conventional comparator sequences across different applications at moderate accelerations [14, 18–24]. Further reading: [25].

Possible limitations

Similar to what is known from iterative reconstructions in computed tomography, CS can lead to an "artificial" image impression when noise reduction is high (i. e., especially at high acceleration). Such images, while low in noise (paradoxical relationship of SNR and acceleration compared to e. g. conventional parallel imaging), potentially exhibit reduced detail detectability [26].

CS sequences may exhibit artefact patterns directly related to undersampling [16, 27]. In addition, artefacts of other causes may appear altered in CS sequences, making them more difficult to classify. We also assume that the artefacts differ between the different implementations. Artefacts to be expected when using a combination of CS and parallel imaging with SENSE have been described in detail [27], including a "wax-layer artefact" with increased inhomogeneities over the image area during motion, streak artefacts and focally-appearing grainy noise [27]. For example, in another CS implementation of a 3 D FLAIR, motion artefacts can lead to cortical signal fluctuations.

In particular, time-of-flight MR angiography (ToF MRA) allows high acceleration factors to be achieved for exclusive arterial vascular imaging [19, 21, 22]. In our experience, however, this can make vessel contours look irregular, thus mimicking potential caliber variations. Usually, ToF MRA as a high-resolution T1-weighted sequence can provide additional information outside the vessels such as detection of wall hematomas [28] as well as (post-contrast) assessment of thrombosis of the cavernous sinus. This extra-arterial information from ToF-MRA might be limited with CS acceleration compared with ToF MRA without CS.

Practical notes on application

In clinical implementations, the user usually has little ability to influence the individual intertwined components that contribute to image formation. For example, settings are combined in an acceleration factor, possibly in conjunction with the possibility to control the strength of noise reduction. For many applications, the literature currently does not yet allow any concrete conclusions to be drawn regarding optimal detailed settings, so that their selection is currently also at the discretion of the respective user, taking into account diagnostic recommendations and guidelines. The accelerated measurement can be used to increase the spatial resolution or to adjust contrast-related parameters so that the contrast between pathologically altered and healthy tissue is increased [15].

Outlook on additional Techniques

Other techniques continue or are increasingly being discussed for clinical use [29]; however, some in earlier stages of development, are primarily used for scientific purposes or are reserved for special indications. For the sake of clarity, only reference is made to the relevant literature with regard to advanced imaging techniques for specific rarer indications. These include clinical functional MRI, diffusion imaging for tractography, spectroscopic imaging, and perfusion imaging as relevant, for example, in preoperative diagnostics for neuronavigation or biopsy planning [30], special techniques to examine the spinal cord [31], oxygenation mapping [32], and synthetic MRI [33, 34] to generate multiple contrasts from a single measurement. Improvements in image quality and acceleration are sought through image reconstruction using artificial intelligence [35]. Finally, MR fingerprinting, which currently has no widespread clinical use, should be mentioned here. In this process, specific tissue parameters are assigned to the relatively "chaotic" recorded temporal signal evolution of a single measurement using a so-called dictionary. Thus, quantitative parameters can also be determined in addition to standard images with different weightings [36, 37]. This may potentially lead to a paradigm shift from single sequences optimized based on visual criteria to a quantitative examination concept in MRI focused on diagnostic accuracy.

Summary Discussion of Applications for Regions of the Nervous System

We would like to conclude by summarizing important potential applications in neuroradiology separately according to typical examination regions. These are suggestions for using the techniques presented in this two-part article to improve the quality of neuroradiological examinations or to optimize diagnostic procedures.

Brain

Near-isotropic 3 D FLAIR sequences with fat suppression and possibly accelerated with CS have particular potential as a uniform cornerstone for almost all cerebral examination protocols. In addition to independence from a specific slice orientation during the examination, the focus is on high lesion detectability and spatial precision, which together also lead to higher comparability between examinations. Multiple sclerosis (MS) stands out as a typical clinical application field for 3D-FLAIR due to advantages in lesion detection and monitoring [38–40]. In addition to good comparability over time, a 3 D FLAIR usually eliminates the need for additional sequences to detect infratentorial lesions [38, 39, 41–43]. The classification of juxtacortical lesions likewise succeeds more clearly than with 2 D techniques [39], since the partial volume effects that occur due to the greater slice thickness and slice gaps in 2 D imaging are reduced. In addition, 3 D FLAIR allows follow-up of brain tumors to detect slow changes in diffusely infiltrating portions even with variable slice angulation [44, 45]. In epilepsy diagnostics, 3 D FLAIR is established for the detection of focal cortical dysplasia [46–48], primarily due to geometric properties [49]. Strength of 3 D FLAIR in cerebral imaging is additionally the often good detectability of extracranial lesions as well as the assessability of basal cisterns and venous sinuses due to low susceptibility to hyperintense flow artefacts. Examples include good detectability of fresh subarachnoid hemorrhages [50] (▶ Fig. 2) or certain venous thrombi (see Part 1).

T2-weighted 3 D TSE sequences are suitable for the assessment of CSF spaces, such as for the assessment of CSF flow in the aqueduct [51]. Since the sequences are less affected by susceptibility artefacts, they are also suitable for patients with shunts.

Depending on the manufacturer, 2 D T2 TSE and DWI should be accelerated by SMS or CS with good image quality, This advantage can be used to arrive at a compromise between speed gain and improved image quality. SMS is suitable for the acquisition of DWI data with a smaller slice thickness, for example for the detection of smaller infarctions (▶ Fig. 3) and lesions in the context of transient global amnesia or for a compromise between acceleration and smaller slice thickness in 2 D T2 TSE. Furthermore, very short emergency protocols have been published using the acceleration procedures mentioned above [52].

T1-weighted 3 D gradient echo sequences (e. g. MPRAGE) are currently favored and helpful when imaging brain tumors [53] to achieve the required small slice thickness for the detection of
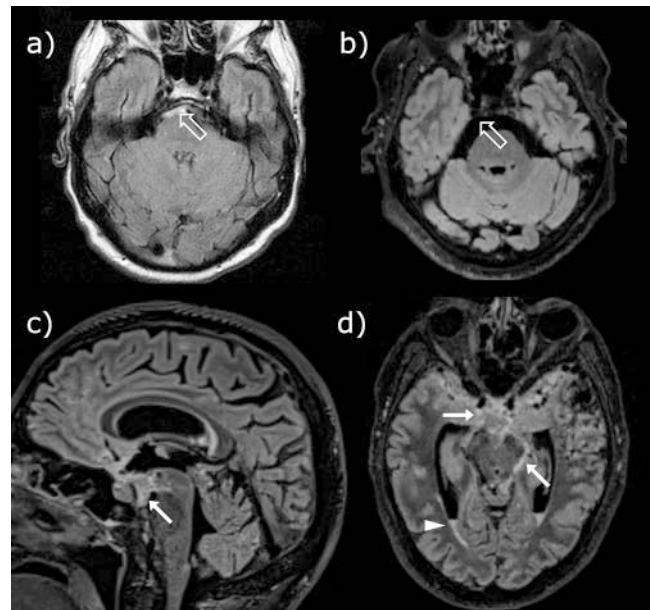

▶ **Fig. 2** Unlike **a)** 2 D FLAIR, **b)** 3 D FLAIR does not usually suffer from flow-related artefacts in the basal cisterns (open arrows). Such artefacts typically impede subarachnoid hemorrhage detection by 2 D FLAIR. **c)** and **d)** 3 D FLAIR in a patient with subarachnoid hemorrhage. Hyperintense appearance of blood in the subarachnoid space (arrows) and in the posterior horns of the lateral ventricles (arrow tip). Lack of complete signal suppression of the cerebrospinal fluid.

brain metastases [54]. Their robustness has increased to the point where the benefits can increasingly outweigh drawbacks such as somewhat limited gadolinium contrast (compared to 2 D SE). However, further development of T1-weighted 3 D TSE sequences remains to be seen, although in the medium term they can assume these roles. In general, T1-weighted 3 D sequences are also suitable for routine applications beyond established indications such as neurooncology, given increasingly higher resolution requirements in guidelines, and can thus help simplify protocol structure.

As an example, a basic protocol for examinations of the brain with a broad scope using several of the techniques presented here is presented in **Online Table 1**.

Cerebral Vessels

ToF MRA can be significantly accelerated with CS for many clinical questions. Flow sensitivity makes T2-weighted 3 D TSE sequences suitable for extension assessment of vascular lesions, for example, arteriovenous malformation (▶ **Fig. 4a**). For the assessment of arterial vessel walls (e. g., vasculitis diagnosis [55–58] (▶ **Fig. 4b**)), T1-weighted 3 D TSE sequences [59] should be used. It should be noted that because of the high sensitivity for vessel wall enhancement, physiological hyperintensities (e. g., approximately 1 cm after dural penetration [59]), as well as enhancement after thrombectomy [60] and predominantly eccentric in intracranial arteriosclerosis [61] can be observed. In modified form, these sequences
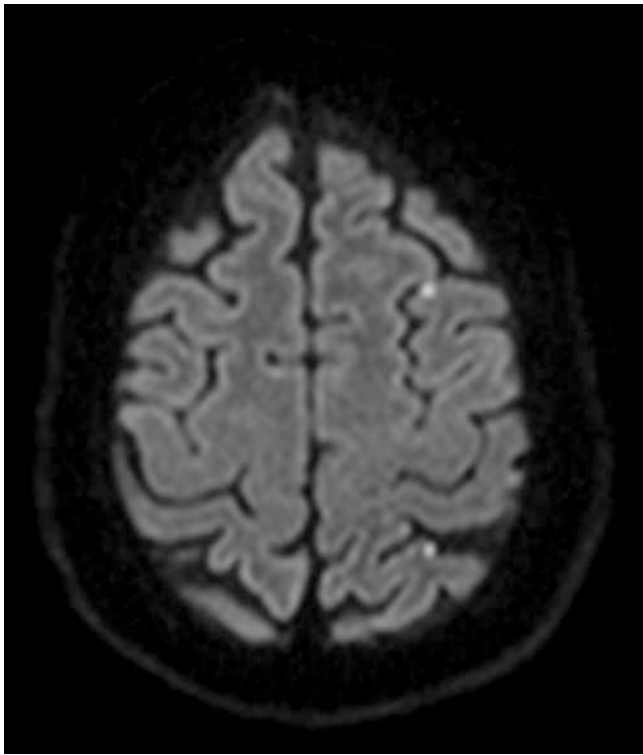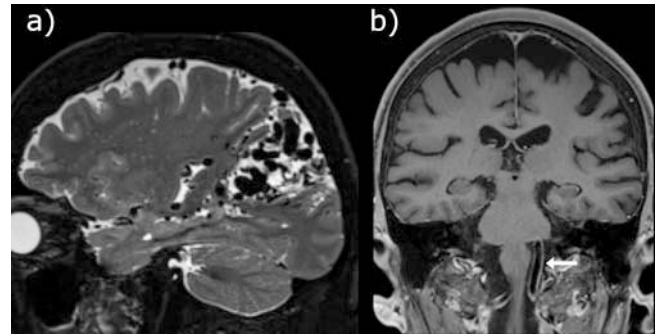
► **Fig. 3** 2 D DWI SE-EPI accelerated with simultaneous mult-slice imaging. This acceleration technique can contribute to relevant acceleration and thus facilitate higher resolution imaging in clinically realistic times. This example (2.5 mm slice thickness at 1.5 T, acquisition duration around 2 minutes) shows high sensitivity for small cortical infarcts.

► **Fig. 4** Vascular applications of 3 D TSE techniques: **a)** 3 D T2 TSE sequence in a patient with an arterio-venous malformation. This technique is particularly useful for assessing the nidus as well as large and medium-sized feeding and draining vessels owing to the possibility of multiplanar reconstructions and its strong flow void susceptibility. Flow voids are enhanced by a relatively low refocusing angle. Such imaging data are also suitable for image fusion with 3 D angiography data. **b)** fat-suppressed 3 D T1 TSE sequence (here: accelerated with compressed sensing, resolution 0.87 mm isotropic at 1.5 T) are utilized for arterial vessel wall imaging. This is made possible by a strong flow void susceptibility. While short segment vessel wall enhancement for approximately 1 cm after crossing the dura is physiological, this example shows longer segment circular enhancement of the vertebral artery (arrow). This is compatible with a diagnosis of cerebral vasculitis.

are also suitable for the detection of dissections [62–66] and could replace more elaborate protocols with multiple single sequences in the future. Furthermore note the often good co-interpretability of large venous vessels in some structural 3 D sequences (FLAIR and T1/MPRAGE) should be noted.

Skull Base, Head and Neck

Decisive improvements in the image quality of fat-suppressed sequences could be achieved in this region with increasing use of Dixon techniques (in combination with various 2 D and 3 D base sequences). They are particularly well suited for imaging the head and neck region with a large field of view (FOV) [67] as well as the brachial plexus [68] because of their insensitivity to field inhomogeneities at anatomic transitions. T1-weighted 3 D gradient-echo sequences with Dixon technique (e. g., VIBE-Dixon) are suitable for high-resolution imaging of the skull base and orbit [29] (► **Fig. 5**), whereas, however, because of the higher gadolinium contrast, TSE sequences appear advantageous for the detection of optic neuritis [69]. Radial fat-suppressed T1-weighted 3 D gradient echo sequences appear equally suitable for routine studies in these regions due to their robustness to motion artefacts [70]. Neuroradiologically, they are particularly suitable for imaging the skull base or orbita [71]. As an alternative to the constructive interference in steady state technique (CISS), particularly

strongly T2-weighted 3 D TSE sequences in combination with driven-equilibrium (DRIVE) techniques for imaging the basal cisterns with cranial nerves and the inner ear structures have already been established for some time [72, 73]. However, they can currently be supplemented by CS to improve measurement time and/or resolution. Touska et al. recently published a detailed review of new MR techniques in the head/neck region [74].

Spinal Column

2 D TSE sequences continue to be the mainstay of imaging of the spine, particularly the spinal cord. Of particular interest here are Dixon techniques, which, depending on their specific settings, can provide various image data simultaneously with high image quality, which can be used, for example, just like fat-saturated and non-fat-saturated images [75–79] (► **Fig. 6**). For T2w (T2 TSE Dixon) in particular, we believe this has proven effective and can often replace Short Tau Inversion Recovery (STIR) acquisitions, simplifying the overall protocol structure. Recent work even claims that using the T2 Dixon fat image, a T1-weighted sequence can also be omitted in degenerative changes [77, 80]. In the spinal application of T2 TSE Dixon, optimization with respect to measurement time, resolution and SNR may be useful, depending on the manufacturer and local requirements. When imaging patients with spondylodesis, metal artefact reduction techniques for visualization of neuroforamina and spinal canal lend themselves to problem solving in individual cases.

For specific issues 3 D techniques can be used complementarily. In spinal imaging, T2-weighted 3 D TSE sequences are suitable for visualizing the spinal canal and neuroforamina [81, 82]
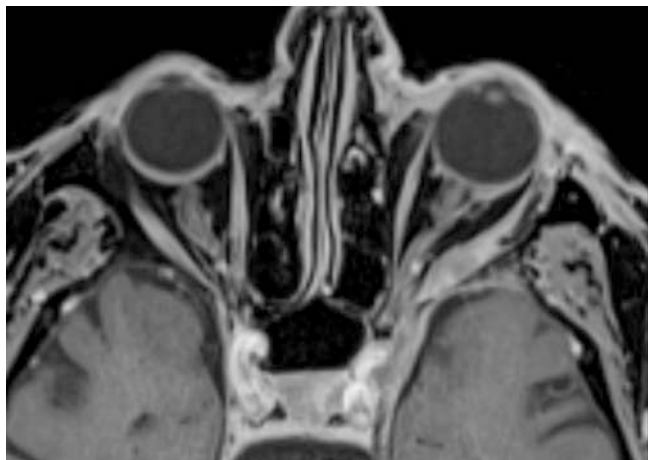
▶ **Fig. 5** 3 D T1 Dixon gradient echo sequence (VIBE Dixon) of the orbits. The Dixon technique helps achieve homogeneous fat suppression even immediately adjacent to the air-filled paranasal sinuses.

and have also been proposed as a screening sequence for this purpose [83, 84]. When additionally combined with fat suppression they can be used for the identification of cerebrospinal fluid leakage [85]. However, they currently appear inferior to 2 D techniques for myelon lesions due to artefacts [86]. Currently, advances in terms of resolution and artefacts in the area of the spinal cord remain to be seen. Experience with CS acceleration in spinal imaging is limited to date, but again suggests potential routine use [87–89].

Peripheral Nervous System

For targeted examination of a short peripheral nerve segment, fat-suppressed 2 D TSE sequences are still important to detect fascicular structure in addition to T2w hyperintensities [90]. In combination with STIR for fat suppression, 3 D TSE sequences are useful for visualizing the plexus [91–94] and conditionally the further course of peripheral nerves [90, 95]. Parameters should thus be optimized to avoid hyperintensity of venous vessels, which could otherwise be mistaken for neuronal structures. This can be achieved by using a low refocus angle [59, 68, 96] and black blood techniques [91, 95]. Metal artefact reduction techniques, for example, can help visualize the sciatic nerve adjacent to hip arthroplasty (▶ **Fig. 5** in Part 1).

Conclusions

The techniques presented in this two-part review can improve MR diagnostics in neuroradiology. They open up new possibilities for standardization or even individualization of examinations as illustrated in this part of the article for different regions of the nervous system. The acceleration techniques SMS and CS presented in this part are examples of such recently-developed methods. Compared to conventional acceleration methods, they sometimes exhibit different artefacts. Knowledge of such specific advantages and disadvantages, the ranges of application as well as pitfalls of
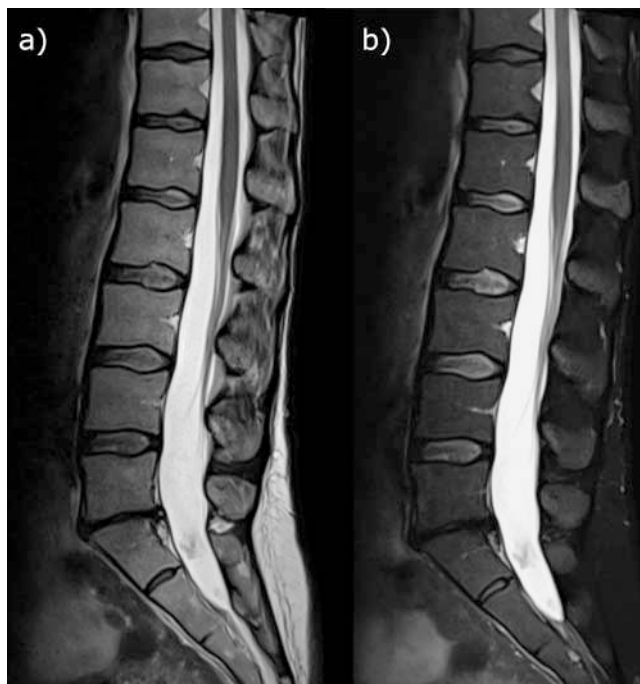
▶ **Fig. 6** 2 D T2 Dixon-TSE sequence of the lumbar spine: **a)** in-phase image, **b)** water image. This technique facilitates time-efficient acquisition of relatively high-resolution images both with and without fat suppression by a single scan. It can thus obviate the need for an additional T2 STIR sequence.

the techniques presented in both parts helps in their successful application in everyday neuroradiological practice.

Conflict of Interest

Christian Mathys: Consulting and lecturing for Siemens on behalf of the employer (Evangelisches Krankenhaus Oldenburg). The other authors declare that they have no conflict of interest.

References

[1] Aja-Fernandez S, Vegas-Sanchez-Ferrero G, Tristan-Vega A. Noise estimation in parallel MRI: GRAPPA and SENSE. Magn Reson Imaging 2014; 32: 281–290. doi:10.1016/j.mri.2013.12.001

[2] Barth M, Breuer F, Koopmans PJ et al. Simultaneous multislice (SMS) imaging techniques. Magn Reson Med 2016; 75: 63–81. doi:10.1002/mrm.25897

[3] Setsompop K, Gagoski BA, Polimeni JR et al. Blipped-controlled aliasing in parallel imaging for simultaneous multislice echo planar imaging with reduced g-factor penalty. Magn Reson Med 2012; 67: 1210–1224. doi:10.1002/mrm.23097

[4] McRobbie DW, Moore EA, Graves MJ. MRI from picture to proton. 3 Aufl. New York: University Printing House, Cambridge University Press; 2017

[5] Risk BB, Kociuba MC, Rowe DB. Impacts of simultaneous multislice acquisition on sensitivity and specificity in fMRI. Neuroimage 2018; 172: 538–553. doi:10.1016/j.neuroimage.2018.01.078

[6] Hsu YC, Chu YH, Tsai SY et al. Simultaneous multi-slice inverse imaging of the human brain. Sci Rep 2017; 7: 17019. doi:10.1038/s41598-017-16976-0

[7] Park S, Chen L, Beckett A et al. Virtual slice concept for improved simultaneous multi-slice MRI employing an extended leakage constraint. Magn Reson Med 2019; 82: 377–386. doi:10.1002/mrm.27741

[8] Xu J, Moeller S, Auerbach EJ et al. Evaluation of slice accelerations using multiband echo planar imaging at 3 T. Neuroimage 2013; 83: 991–1001. doi:10.1016/j.neuroimage.2013.07.055

[9] Setsompop K, Cohen-Adad J, Gagoski BA et al. Improving diffusion MRI using simultaneous multi-slice echo planar imaging. Neuroimage 2012; 63: 569–580. doi:10.1016/j.neuroimage.2012.06.033

[10] Todd N, Moeller S, Auerbach EJ et al. Evaluation of 2D multiband EPI imaging for high-resolution, whole-brain, task-based fMRI studies at 3T: Sensitivity and slice leakage artifacts. Neuroimage 2016; 124: 32–42. doi:10.1016/j.neuroimage.2015.08.056

[11] Miller KL, Alfaro-Almagro F, Bangerter NK et al. Multimodal population brain imaging in the UK Biobank prospective epidemiological study. Nat Neurosci 2016; 19: 1523–1536. doi:10.1038/nn.4393

[12] Smith SM, Beckmann CF, Andersson J et al. Resting-state fMRI in the Human Connectome Project. Neuroimage 2013; 80: 144–168. doi:10.1016/j.neuroimage.2013.05.039

[13] Fritz J, Fritz B, Zhang J et al. Simultaneous Multislice Accelerated Turbo Spin Echo Magnetic Resonance Imaging: Comparison and Combination With In-Plane Parallel Imaging Acceleration for High-Resolution Magnetic Resonance Imaging of the Knee. Invest Radiol 2017; 52: 529–537. doi:10.1097/RLI.0000000000000376

[14] Monch S, Sollmann N, Hock A et al. Magnetic Resonance Imaging of the Brain Using Compressed Sensing – Quality Assessment in Daily Clinical Routine. Clin Neuroradiol 2020; 30: 279–286. doi:10.1007/s00062-019-00789-x

[15] Lustig M, Donoho D, Pauly JM. Sparse MRI: The application of compressed sensing for rapid MR imaging. Magn Reson Med 2007; 58: 1182–1195. doi:10.1002/mrm.21391

[16] Geethanath S, Reddy R, Konar AS et al. Compressed sensing MRI: a review. Crit Rev Biomed Eng 2013; 41: 183–204. doi:10.1615/critrevbiomedeng.2014008058

[17] Kayvanrad M, Lin A, Joshi R et al. Diagnostic quality assessment of compressed sensing accelerated magnetic resonance neuroimaging. J Magn Reson Imaging 2016; 44: 433–444. doi:10.1002/jmri.25149

[18] Vranic JE, Cross NM, Wang Y et al. Compressed Sensing-Sensitivity Encoding (CS-SENSE) Accelerated Brain Imaging: Reduced Scan Time without Reduced Image Quality. AJNR Am J Neuroradiol 2019; 40: 92–98. doi:10.3174/ajnr.A5905

[19] Lu SS, Qi M, Zhang X et al. Clinical Evaluation of Highly Accelerated Compressed Sensing Time-of-Flight MR Angiography for Intracranial Arterial Stenosis. AJNR Am J Neuroradiol 2018; 39: 1833–1838. doi:10.3174/ajnr.A5786

[20] Yamamoto T, Okada T, Fushimi Y et al. Magnetic resonance angiography with compressed sensing: An evaluation of moyamoya disease. PLoS One 2018; 13: e0189493. doi:10.1371/journal.pone.0189493

[21] Fushimi Y, Fujimoto K, Okada T et al. Compressed Sensing 3-Dimensional Time-of-Flight Magnetic Resonance Angiography for Cerebral Aneurysms: Optimization and Evaluation. Invest Radiol 2016; 51: 228–235. doi:10.1097/RLI.0000000000000226

[22] Fushimi Y, Okada T, Kikuchi T et al. Clinical evaluation of time-of-flight MR angiography with sparse undersampling and iterative reconstruction for cerebral aneurysms. NMR Biomed 2017; 30. doi:10.1002/nbm.3774

[23] Toledano-Massiah S, Sayadi A, de Boer R et al. Accuracy of the Compressed Sensing Accelerated 3D-FLAIR Sequence for the Detection of MS Plaques at 3T. AJNR Am J Neuroradiol 2018; 39: 454–458. doi:10.3174/ajnr.A5517

[24] Delattre BMA, Boudabbous S, Hansen C et al. Compressed sensing MRI of different organs: ready for clinical daily practice? Eur Radiol 2020; 30: 308–319. doi:10.1007/s00330-019-06319-0

[25] Feng L, Benkert T, Block KT et al. Compressed sensing for body MRI. J Magn Reson Imaging 2017; 45: 966–987. doi:10.1002/jmri.25547

[26] Sharma SD, Fong CL, Tzung BS et al. Clinical image quality assessment of accelerated magnetic resonance neuroimaging using compressed sensing. Invest Radiol 2013; 48: 638–645. doi:10.1097/RLI.0b013e31828a012d

[27] Sartoretti T, Reischauer C, Sartoretti E et al. Common artefacts encountered on images acquired with combined compressed sensing and SENSE. Insights Imaging 2018; 9: 1107–1115. doi:10.1007/s13244-018-0668-4

[28] Renard D, Delorme M, Castelnovo G. Hyperintense intramural hematoma on time-of-flight sequences in carotid dissection. Eur Neurol 2013; 70: 141. doi:10.1159/000351351

[29] Viallon M, Cuvinciuc V, Delattre B et al. State-of-the-art MRI techniques in neuroradiology: principles, pitfalls, and clinical applications. Neuroradiology 2015; 57: 441–467. doi:10.1007/s00234-015-1500-1

[30] Villanueva-Meyer JE, Mabray MC, Cha S. Current Clinical Brain Tumor Imaging. Neurosurgery 2017; 81: 397–415. doi:10.1093/neuros/nyx103

[31] Martin AR, Aleksanderek I, Cohen-Adad J et al. Translating state-of-the-art spinal cord MRI techniques to clinical use: A systematic review of clinical studies utilizing DTI, MT, MWF, MRS, and fMRI. Neuroimage Clin 2016; 10: 192–238. doi:10.1016/j.nicl.2015.11.019

[32] Christen T, Bolar DS, Zaharchuk G. Imaging brain oxygenation with MRI using blood oxygenation approaches: methods, validation, and clinical applications. AJNR Am J Neuroradiol 2013; 34: 1113–1123. doi:10.3174/ajnr.A3070

[33] Ji S, Yang D, Lee J et al. Synthetic MRI: Technologies and Applications in Neuroradiology. J Magn Reson Imaging 2020. doi:10.1002/jmri.27440

[34] Hagiwara A, Warntjes M, Hori M et al. SyMRI of the Brain: Rapid Quantification of Relaxation Rates and Proton Density, With Synthetic MRI, Automatic Brain Segmentation, and Myelin Measurement. Invest Radiol 2017; 52: 647–657. doi:10.1097/RLI.0000000000000365

[35] Lin DJ, Johnson PM, Knoll F et al. Artificial Intelligence for MR Image Reconstruction: An Overview for Clinicians. J Magn Reson Imaging 2021; 53: 1015–1028. doi:10.1002/jmri.27078

[36] Poorman ME, Martin MN, Ma D et al. Magnetic resonance fingerprinting Part 1: Potenzial uses, current challenges, and recommendations. J Magn Reson Imaging 2020; 51: 675–692. doi:10.1002/jmri.26836

[37] McGivney DF, Boyacioglu R, Jiang Y et al. Magnetic resonance fingerprinting review part 2: Technique and directions. J Magn Reson Imaging 2020; 51: 993–1007. doi:10.1002/jmri.26877

[38] Rovira A, Wattjes MP, Tintore M et al. Evidence-based guidelines: MAGNIMS consensus guidelines on the use of MRI in multiple sclerosis-clinical implementation in the diagnostic process. Nat Rev Neurol 2015; 11: 471–482. doi:10.1038/nrneurol.2015.106

[39] Filippi M, Preziosa P, Banwell BL et al. Assessment of lesions on magnetic resonance imaging in multiple sclerosis: practical guidelines. Brain 2019; 142: 1858–1875. doi:10.1093/brain/awz144

[40] Traboulsee A, Simon JH, Stone L et al. Revised Recommendations of the Consortium of MS Centers Task Force for a Standardized MRI Protocol and Clinical Guidelines for the Diagnosis and Follow-Up of Multiple Sclerosis. AJNR Am J Neuroradiol 2016; 37: 394–401. doi:10.3174/ajnr.A4539

[41] Wang KY, Uribe TA, Lincoln CM. Comparing lesion detection of infratentorial multiple sclerosis lesions between T2-weighted spin-echo, 2D-FLAIR, and 3D-FLAIR sequences. Clin Imaging 2018; 51: 229–234. doi:10.1016/j.clinimag.2018.05.017

[42] Lecler A, El Sanharawi I, El Methni J et al. Improving Detection of Multiple Sclerosis Lesions in the Posterior Fossa Using an Optimized 3D-FLAIR Sequence at 3T. AJNR Am J Neuroradiol 2019; 40: 1170–1176. doi:10.3174/ajnr.A6107

[43] Tomassini V, Sinclair A, Sawlani V et al. Diagnosis and management of multiple sclerosis: MRI in clinical practice. J Neurol 2020; 267: 2917–2925. doi:10.1007/s00415-020-09930-0

[44] Sollmann N, Gutbrod-Fernandez M, Burian E et al. Subtraction Maps Derived from Longitudinal Magnetic Resonance Imaging in Patients with Glioma Facilitate Early Detection of Tumor Progression. Cancers (Basel) 2020; 12. doi:10.3390/cancers12113111

[45] Huber T, Alber G, Bette S et al. Reliability of Semi-Automated Segmentations in Glioblastoma. Clin Neuroradiol 2017; 27: 153–161. doi:10.1007/s00062-015-0471-2

[46] Mellerio C, Labeyrie MA, Chassoux F et al. Optimizing MR imaging detection of type 2 focal cortical dysplasia: best criteria for clinical practice. AJNR Am J Neuroradiol 2012; 33: 1932–1938. doi:10.3174/ajnr.A3081

[47] Urbach H, Mast H, Egger K et al. Presurgical MR Imaging in Epilepsy. Clin Neuroradiol 2015; 25 (Suppl. 2): 151–155. doi:10.1007/s00062-015-0387-x

[48] Saini J, Singh A, Kesavadas C et al. Role of three-dimensional fluid-attenuated inversion recovery (3D FLAIR) and proton density magnetic resonance imaging for the detection and evaluation of lesion extent of focal cortical dysplasia in patients with refractory epilepsy. Acta Radiol 2010; 51: 218–225. doi:10.3109/02841850903433805

[49] Tschampa HJ, Urbach H, Malter M et al. Magnetic resonance imaging of focal cortical dysplasia: Comparison of 3D and 2D fluid attenuated inversion recovery sequences at 3T. Epilepsy Res 2015; 116: 8–14. doi:10.1016/j.eplepsyres.2015.07.004

[50] Lummel N, Schoepf V, Burke M et al. 3D fluid-attenuated inversion recovery imaging: reduced CSF artifacts and enhanced sensitivity and specificity for subarachnoid hemorrhage. AJNR Am J Neuroradiol 2011; 32: 2054–2060. doi:10.3174/ajnr.A2682

[51] Algin O, Turkbey B. Evaluation of aqueductal stenosis by 3D sampling perfection with application-optimized contrasts using different flip angle evolutions sequence: preliminary results with 3T MR imaging. AJNR Am J Neuroradiol 2012; 33: 740–746. doi:10.3174/ajnr.A2833

[52] Wenger KJ, Hattingen E. Schnelle MRT-Sequenzen für die akute neurologische Abklärung. Der Radiologe 2020; 60: 208–215. doi:10.1007/s00117-020-00649-7

[53] Ellingson BM, Bendszus M, Boxerman J et al. Consensus recommendations for a standardized Brain Tumor Imaging Protocol in clinical trials. Neuro Oncol 2015; 17: 1188–1198. doi:10.1093/neuonc/nov095

[54] Kaufmann TJ, Smits M, Boxerman J et al. Consensus recommendations for a standardized brain tumor imaging protocol for clinical trials in brain metastases. Neuro Oncol 2020; 22: 757–772. doi:10.1093/neuonc/noaa030

[55] Eiden S, Beck C, Venhoff N et al. High-resolution contrast-enhanced vessel wall imaging in patients with suspected cerebral vasculitis: Prospective comparison of whole-brain 3D T1 SPACE versus 2D T1 black blood MRI at 3 Tesla. PLoS One 2019; 14: e0213514. doi:10.1371/journal.pone.0213514

[56] Zeiler SR, Qiao Y, Pardo CA et al. Vessel Wall MRI for Targeting Biopsies of Intracranial Vasculitis. AJNR Am J Neuroradiol 2018; 39: 2034–2036. doi:10.3174/ajnr.A5801

[57] Poillon G, Collin A, Benhamou Y et al. Increased diagnostic accuracy of giant cell arteritis using three-dimensional fat-saturated contrast-enhanced vessel-wall magnetic resonance imaging at 3 T. Eur Radiol 2020; 30: 1866–1875. doi:10.1007/s00330-019-06536-7

[58] Wang LJ, Kong DZ, Guo ZN et al. Study on the Clinical, Imaging, and Pathological Characteristics of 18 Cases with Primary Central Nervous System Vasculitis. J Stroke Cerebrovasc Dis 2019; 28: 920–928. doi:10.1016/j.jstrokecerebrovasdis.2018.12.007

[59] Lindenholz A, van der Kolk AG, Zwanenburg JJM et al. The Use and Pitfalls of Intracranial Vessel Wall Imaging: How We Do It. Radiology 2018; 286: 12–28. doi:10.1148/radiol.2017162096

[60] Lindenholz A, van der Schaaf IC, van der Kolk AG et al. MRI Vessel Wall Imaging after Intra-Arterial Treatment for Acute Ischemic Stroke. AJNR Am J Neuroradiol 2020; 41: 624–631. doi:10.3174/ajnr.A6460

[61] Mossa-Basha M, Watase H, Sun J et al. Inter-rater and scan-rescan reproducibility of the detection of intracranial atherosclerosis on contrast-enhanced 3D vessel wall MRI. Br J Radiol 2019; 92: 20180973. doi:10.1259/bjr.20180973

[62] Luo Y, Guo ZN, Niu PP et al. 3D T1-weighted black blood sequence at 3.0 Tesla for the diagnosis of cervical artery dissection. Stroke Vasc Neurol 2016; 1: 140–146. doi:10.1136/svn-2016-000028

[63] Takano K, Yamashita S, Takemoto K et al. MRI of intracranial vertebral artery dissection: evaluation of intramural haematoma using a black blood, variable-flip-angle 3D turbo spin-echo sequence. Neuroradiology 2013; 55: 845–851. doi:10.1007/s00234-013-1183-4

[64] Edjlali M, Roca P, Rabrait C et al. 3D fast spin-echo T1 black-blood imaging for the diagnosis of cervical artery dissection. AJNR Am J Neuroradiol 2013; 34: E103–E106. doi:10.3174/ajnr.A3261

[65] Ogawa M, Omata S, Kan H et al. Utility of the variable flip angle 3D fast-spin echo (isoFSE) sequence on 3T MR for diagnosing vertebrobasilar artery dissection. Radiol Phys Technol 2018; 11: 228–234. doi:10.1007/s12194-018-0460-7

[66] Sakurai K, Miura T, Sagisaka T et al. Evaluation of luminal and vessel wall abnormalities in subacute and other stages of intracranial vertebrobasilar artery dissections using the volume isotropic turbo-spin-echo acquisition (VISTA) sequence: a preliminary study. J Neuroradiol 2013; 40: 19–28. doi:10.1016/j.neurad.2012.02.005

[67] Gaddikeri S, Mossa-Basha M, Andre JB et al. Optimal Fat Suppression in Head and Neck MRI: Comparison of Multipoint Dixon with 2 Different Fat-Suppression Techniques, Spectral Presaturation and Inversion Recovery, and STIR. AJNR Am J Neuroradiol 2018; 39: 362–368. doi:10.3174/ajnr.A5483

[68] Wang X, Harrison C, Mariappan YK et al. MR Neurography of Brachial Plexus at 3.0 T with Robust Fat and Blood Suppression. Radiology 2017; 283: 538–546. doi:10.1148/radiol.2016152842

[69] Berg S, Kaschka I, Utz KS et al. Baseline magnetic resonance imaging of the optic nerve provides limited predictive information on short-term recovery after acute optic neuritis. PLoS One 2015; 10: e0113961. doi:10.1371/journal.pone.0113961

[70] Wu X, Raz E, Block TK et al. Contrast-enhanced radial 3D fat-suppressed T1-weighted gradient-recalled echo sequence versus conventional fat-suppressed contrast-enhanced T1-weighted studies of the head and neck. Am J Roentgenol 2014; 203: 883–889. doi:10.2214/Am J Roentgenol.13.11729

[71] Bangiyev L, Raz E, Block TK et al. Evaluation of the orbit using contrast-enhanced radial 3D fat-suppressed T1 weighted gradient echo (Radial-VIBE) sequence. Br J Radiol 2015; 88: 20140863. doi:10.1259/bjr.20140863

[72] Ciftci E, Anik Y, Arslan A et al. Driven equilibrium (drive) MR imaging of the cranial nerves V-VIII: comparison with the T2-weighted 3D TSE sequence. Eur J Radiol 2004; 51: 234–240. doi:10.1016/j.ejrad.2003.10.019

[73] Savvas E, Heslinga K, Sundermann B et al. Prognostic factors in cochlear implantation in adults: Determining central process integrity. Am J Otolaryngol 2020; 41: 102435. doi:10.1016/j.amjoto.2020.102435

[74] Touska P, Connor SEJ. Recent advances in MRI of the head and neck, skull base and cranial nerves: new and evolving sequences, analyses and clinical applications. Br J Radiol 2019; 92: 20190513. doi:10.1259/bjr.20190513

[75] Pokorney AL, Chia JM, Pfeifer CM et al. Improved fat-suppression homogeneity with mDIXON turbo spin echo (TSE) in pediatric spine imaging at 3.0 T. Acta Radiol 2017; 58: 1386–1394. doi:10.1177/0284185117690424

[76] Guerini H, Omoumi P, Guichoux F et al. Fat Suppression with Dixon Techniques in Musculoskeletal Magnetic Resonance Imaging: A Pictorial Review. Semin Musculoskelet Radiol 2015; 19: 335–347. doi:10.1055/s-0035-1565913

[77] Zanchi F, Richard R, Hussami M et al. MRI of non-specific low back pain and/or lumbar radiculopathy: do we need T1 when using a sagittal T2-weighted Dixon sequence? Eur Radiol 2020; 30: 2583–2593. doi:10.1007/s00330-019-06626-6

[78] Low RN, Austin MJ, Ma J. Fast spin-echo triple echo dixon: Initial clinical experience with a novel pulse sequence for simultaneous fat-suppressed and nonfat-suppressed T2-weighted spine magnetic resonance imaging. J Magn Reson Imaging 2011; 33: 390–400. doi:10.1002/jmri.22453

[79] Brandao S, Seixas D, Ayres-Basto M et al. Comparing T1-weighted and T2-weighted three-point Dixon technique with conventional T1-weighted fat-saturation and short-tau inversion recovery (STIR) techniques for the study of the lumbar spine in a short-bore MRI machine. Clin Radiol 2013; 68: e617–e623. doi:10.1016/j.crad.2013.06.004

[80] Maeder Y, Dunet V, Richard R et al. Bone Marrow Metastases: T2-weighted Dixon Spin-Echo Fat Images Can Replace T1-weighted Spin-Echo Images. Radiology 2018; 286: 948–959. doi:10.1148/radiol.2017170325

[81] Chokshi FH, Sadigh G, Carpenter W et al. Diagnostic Quality of 3D T2-SPACE Compared with T2-FSE in the Evaluation of Cervical Spine MRI Anatomy. AJNR Am J Neuroradiol 2017; 38: 846–850. doi:10.3174/ajnr.A5080

[82] Hossein J, Fariborz F, Mehrnaz R et al. Evaluation of diagnostic value and T2-weighted three-dimensional isotropic turbo spin-echo (3D-SPACE) image quality in comparison with T2-weighted two-dimensional turbo spin-echo (2D-TSE) sequences in lumbar spine MR imaging. Eur J Radiol Open 2019; 6: 36–41. doi:10.1016/j.ejro.2018.12.003

[83] Koontz NA, Wiggins RH 3rd et al. Less Is More: Efficacy of Rapid 3D-T2 SPACE in ED Patients with Acute Atypical Low Back Pain. Acad Radiol 2017; 24: 988–994. doi:10.1016/j.acra.2017.02.011

[84] Sayah A, Jay AK, Toaff JS et al. Effectiveness of a Rapid Lumbar Spine MRI Protocol Using 3D T2-Weighted SPACE Imaging Versus a Standard Protocol for Evaluation of Degenerative Changes of the Lumbar Spine. Am J Roentgenol 2016; 207: 614–620. doi:10.2214/Am J Roentgenol.15.15764

[85] Dobrocky T, Winklehner A, Breiding PS et al. Spine MRI in Spontaneous Intracranial Hypotension for CSF Leak Detection: Nonsuperiority of Intrathecal Gadolinium to Heavily T2-Weighted Fat-Saturated Sequences. AJNR Am J Neuroradiol 2020; 41: 1309–1315. doi:10.3174/ajnr.A6592

[86] Vargas MI, Dietemann JL. 3D T2-SPACE versus T2-FSE or T2 Gradient Recalled-Echo: Which Is the Best Sequence? AJNR Am J Neuroradiol 2017; 38: E48–E49. doi:10.3174/ajnr.A5190

[87] Bratke G, Rau R, Kabbasch C et al. Speeding up the clinical routine: Compressed sensing for 2D imaging of lumbar spine disc herniation. Eur J Radiol 2021; 140: 109738. doi:10.1016/j.ejrad.2021.109738

[88] Morita K, Nakaura T, Maruyama N et al. Hybrid of Compressed Sensing and Parallel Imaging Applied to Three-dimensional Isotropic T2-weighted Turbo Spin-echo MR Imaging of the Lumbar Spine. Magn Reson Med Sci 2020; 19: 48–55. doi:10.2463/mrms.mp.2018-0132

[89] Bratke G, Rau R, Weiss K et al. Accelerated MRI of the Lumbar Spine Using Compressed Sensing: Quality and Efficiency. J Magn Reson Imaging 2019; 49: e164–e175. doi:10.1002/jmri.26526

[90] Chhabra A, Andreisek G, Soldatos T et al. MR neurography: past, present, and future. Am J Roentgenol 2011; 197: 583–591. doi:10.2214/Am J Roentgenol.10.6012

[91] Klupp E, Cervantes B, Sollmann N et al. Improved Brachial Plexus Visualization Using an Adiabatic iMSDE-Prepared STIR 3D TSE. Clin Neuroradiol 2019; 29: 631–638. doi:10.1007/s00062-018-0706-0

[92] Viallon M, Vargas MI, Jlassi H et al. High-resolution and functional magnetic resonance imaging of the brachial plexus using an isotropic 3D T2 STIR (Short Term Inversion Recovery) SPACE sequence and diffusion tensor imaging. Eur Radiol 2008; 18: 1018–1023. doi:10.1007/s00330-007-0834-4

[93] Chhabra A, Thawait GK, Soldatos T et al. High-resolution 3T MR neurography of the brachial plexus and its branches, with emphasis on 3D imaging. AJNR Am J Neuroradiol 2013; 34: 486–497. doi:10.3174/ajnr.A3287

[94] Soldatos T, Andreisek G, Thawait GK et al. High-resolution 3-T MR neurography of the lumbosacral plexus. Radiographics 2013; 33: 967–987. doi:10.1148/rg.334115761

[95] Van der Cruyssen F, Croonenborghs TM, Hermans R et al. 3D Cranial Nerve Imaging, a Novel MR Neurography Technique Using Black-Blood STIR TSE with a Pseudo Steady-State Sweep and Motion-Sensitized Driven Equilibrium Pulse for the Visualization of the Extraforaminal Cranial Nerve Branches. AJNR Am J Neuroradiol 2020. doi:10.3174/ajnr.A6904

[96] Mugler JP 3rd. Optimized three-dimensional fast-spin-echo MRI. J Magn Reson Imaging 2014; 39: 745–767. doi:10.1002/jmri.24542